Comparative analysis of *Wolbachia* maternal transmission and localization in host ovaries

Michael T.J. Hague[a,#], Timothy B. Wheeler[b], Brandon S. Cooper[b]

[a]Biology Department
University of Scranton
800 Linden Street
Scranton, PA 18510

[b]Division of Biological Sciences
University of Montana
32 Campus Dr.
Missoula, MT 59812

[#]Corresponding Author
Michael T.J. Hague
Biology Department, Loyola Science Center
800 Linden Street, University of Scranton
Scranton, PA 18510
(570) 941-7962
michael.hague@scranton.edu

ABSTRACT

Many insects and other animals carry microbial endosymbionts that influence their reproduction and fitness. These relationships only persist if endosymbionts are reliably transmitted from one host generation to the next. *Wolbachia* are maternally transmitted endosymbionts found in most insect species, but transmission rates can vary across environments. Maternal transmission of *w*Mel *Wolbachia* depends on temperature in natural *Drosophila melanogaster* hosts and in transinfected *Aedes aegypti*, where *w*Mel is used to block pathogens that cause human disease. In *D. melanogaster*, *w*Mel transmission declines in the cold as *Wolbachia* become less abundant in host ovaries and at the posterior pole plasm (the site of germline formation) in mature oocytes. Here, we assess how temperature affects maternal transmission and underlying patterns of *Wolbachia* localization across 10 *Wolbachia* strains diverged up to 50 million years—including strains closely related to *w*Mel—and their natural *Drosophila* hosts. Many *Wolbachia* maintain high transmission rates across temperatures, despite highly variable (and sometimes low) levels of *Wolbachia* in the ovaries and at the developing germline in late-stage oocytes. Identifying strains like closely related *w*Mel-like *Wolbachia* with stable transmission across variable environmental conditions may improve the efficacy of *Wolbachia*-based biocontrol efforts as they expand into globally diverse environments.

KEYWORDS: *w*Mel, *Drosophila*, host-microbe interaction, vertical transmission

INTRODUCTION

Microbes form diverse relationships with host organisms that span the tree of life, including animals, plants, and protists. Endosymbiosis is an especially close relationship where microbes occupy eukaryotic host cells. Heritable endosymbionts are particularly common in insects[1–3], and these relationships alter fundamental aspects of host biology, including reproduction[4,5], protection for natural enemies[6–9], and nutrient acquisition[10–12].

Many endosymbionts rely on vertical-maternal transmission to spread and persist in insect populations[13–15]. In obligate relationships, these endosymbionts must be maternally transmitted to ensure host survival (e.g., *Buchnera* and aphids[16]). For facultative endosymbionts like *Wolbachia*, imperfect maternal transmission decreases the prevalence of *Wolbachia*-positive individuals within the host population each generation[17–21]. Thus, maternal transmission is a fundamental determinant of how endosymbionts spread, persist, and evolve in host populations[17,22,23]. In addition, the efficacy of *Wolbachia*-based programs to control human diseases[24–26] and agricultural pests[27,28] explicitly requires efficient maternal transmission. This includes introducing the pathogen-blocking *w*Mel *Wolbachia* strain from *Drosophila melanogaster* into mosquito populations to reduce the incidence of dengue and other diseases on multiple continents[29–32]. Nonetheless, it is largely unknown why maternal transmission may breakdown under certain circumstances, especially for non-model systems[15,21,33–36].

Maternal transmission is predicted to depend on endosymbiont density (titer) in female reproductive tissues, and specifically at the site of germline formation during oogenesis[14]. In insects, endosymbionts often achieve vertical transmission by occupying the female ovaries. Endosymbionts are observed in germline stem cells in female hosts where they maintain a tight association with the germline throughout oogenesis, thereby ensuring a germline-to-germline route of vertical transmission through the host matriline[14,15,36,37]. In a more circuitous route, some endosymbionts may also colonize the germline from neighboring somatic cells via cell-to-cell migration through a soma-to-germline route of transmission[4,14,15,38,39]. Our canonical understanding of these cellular processes—and their contributions to maternal transmission—are based almost entirely in the context of standard laboratory conditions where maternal transmission rates are near perfect or perfect[18,20,21,40]. However, maternal transmission of facultative endosymbionts is often imperfect in natural host populations[19,20,41,42] and the cellular processes that lead to transmission breakdown under natural conditions are generally

52 unresolved[21,36]. Understanding why transmission breaks down under certain conditions is critical
53 for predicting endosymbiont spread in nature and improving *Wolbachia*-based biocontrol
54 programs[25,33,34,43].

55 Maternally transmitted *Wolbachia* are the most common endosymbionts on earth,
56 associating with about half of all insect species, as well as other arthropods and nematodes[4,44–46].
57 *Wolbachia* are primarily maternally (vertically) transmitted via the host germline within host
58 species; although, host switching via horizonal transfer between host species is common on
59 evolutionary timescales[47–54]. *Wolbachia* generally form facultative relationships (from the host
60 perspective) in insects, with some individuals in the host population that do not carry *Wolbachia*
61 due to imperfect maternal transmission. Maternal transmission is perhaps the most important
62 determinant of *Wolbachia* prevalence in host populations: theory demonstrates that *Wolbachia*
63 frequency dynamics and equilibria are approximated by the degree of imperfect maternal
64 transmission (μ), the relative fitness (e.g., fecundity) of females with *Wolbachia* (F), and the
65 strength of *Wolbachia*-induced cytoplasmic incompatibility (s_h)[17,55]. Some *Wolbachia* strains
66 (e.g., *w*Ri in *D. simulans*) cause cytoplasmic incompatibility (CI), a crossing incompatibility that
67 generates a frequency-dependent advantage for females with *Wolbachia*[5,56].

68 The prevalence of different *Wolbachia* strains varies widely among host systems, which
69 may be partially explained by differences in maternal transmission rates. For instance, the strong
70 CI-causing *w*Ri strain is observed at high frequencies in global *D. simulans* populations[17,18,57],
71 whereas the weak CI-causing *w*Mel strain is found at intermediate, fluctuating frequencies in *D.*
72 *melanogaster*[58]. *w*Ri frequencies can be plausibly explained by strong CI that causes spread to
73 high frequencies, whereas lower, variable *w*Mel frequencies can be plausibly explained by
74 maternal transmission breakdown as temperatures decrease, in addition to a minimal influence of
75 CI[21]. The thermal sensitivity of maternal transmission may be a feature of *w*Mel, given that heat
76 stress also reduces *w*Mel transmission in transinfected *Aedes aegypti* hosts[33,34,43]. Identifying
77 *Wolbachia* variants that are efficiently transmitted across environmental conditions could
78 potentially contribute to improving the efficacy of *Wolbachia* based biocontrol of human
79 diseases and agricultural pests[25,26].

80 What might underlie variable maternal transmission rates? Maternal transmission
81 breakdown is predicted to stem from reductions in *Wolbachia* abundance and localization
82 throughout host development and specifically at the critical stages of oogenesis thought to

83 facilitate germline-to-germline maternal transmission[14,15,21,36,59–63]. *w*Mel cells are present in the
84 germline stem cells of adult females, and over the course of oogenesis, *w*Mel localize via
85 kinesin-mediated transport to the pole plasm—the site of germline formation—at the posterior
86 cortex of the developing oocyte. In late oogenesis (stage 10), *w*Mel *Wolbachia* display a pattern
87 of posterior localization in oocytes, which is considered to be a key step in the process of
88 germline-to-germline maternal transmission under standard laboratory conditions[14,50,59–63]. In
89 support of this, we recently demonstrated that declining *w*Mel transmission in the cold covaries
90 with a significant reduction in cellular *Wolbachia* abundance at the posterior cortex of stage 10
91 oocytes, which can plausibly explain why maternal transmission is thermally sensitive[21].
92 Outside of the *w*Mel strain, it is unclear how temperature influences *Wolbachia* maternal
93 transmission and posterior localization in stage 10 oocytes for other diverse *Wolbachia*-host
94 associations[15,20]. Under standard 25°C conditions, divergent *Wolbachia* strains exhibit highly
95 variable patterns of localization to the pole plasm at the posterior cortex of stage 10 oocytes of
96 *Drosophila* species, deviating from our canonical understanding of *w*Mel[15]. These patterns range
97 from strongly localized (e.g., *w*Ana in *D. anannassae*) to a complete lack of localization (e.g.,
98 *w*Tri in *D. triauraria*) at the site of germline formation. Some strains, particularly the divergent
99 B-group *w*Mau strain, also exhibit evidence for an alternative soma-to-germline route of
100 transmission, whereby *Wolbachia* in somatically derived follicle cells may invade the oocyte via
101 cell-to-cell migration. It is entirely unknown whether the diverse localization patterns of these
102 *Wolbachia* strains influence rates of maternal transmission and/or are sensitive to thermal
103 perturbation like *w*Mel.
104 Here, we examine temperature effects on *Wolbachia* maternal transmission and
105 localization in host tissues across 10 divergent *Wolbachia* strains naturally found in eight
106 *Drosophila* host species within the *melanogaster* species group (Figure 1, Table S1). These
107 *Wolbachia* comprise nine A-group *Wolbachia*—including closely related *w*Mel-like strains
108 (*w*Mel, *w*MelCS, *w*Seg in *D. seguyi*, and *w*Cha in *D. chauvacae*) and closely related *w*Ri-like
109 strains (*w*Ri, *w*Ana in *D. ananassae*, *w*Aura in *D. auraria*, and *w*Tri in *D. triauraria*)[20,51,53]—and
110 divergent B-group *w*Mau in *D. mauritiana* that diverged up to 46 million years ago from the
111 other A-group strains[40]. We reared flies at 25° and 20°C and then measured maternal
112 transmission rates in conjunction with *Wolbachia* densities (titer) at the tissue level in female
113 ovaries and the remaining somatic tissues. We then used confocal microscopy to examine how

114 temperature impacts the cellular abundance of *Wolbachia* at the site of germline formation at the
115 posterior cortex of stage 10 oocytes during oogenesis. Our results reveal diverse patterns of
116 localization in ovary tissues and late-stage oocytes that are temperature-dependent, but only
117 weakly predictive of maternal transmission rates. We also identify *Wolbachia* strains that are
118 transmitted efficiently regardless of temperature.
119
120 **RESULTS**
121 We estimated the mean rate of maternal transmission (± BC_a confidence intervals) for
122 each *Wolbachia*-host genotype at 25° and 20°C by pairing individual virgin females with
123 *Wolbachia*-free males (see Methods), allowing the females to lay for eight days, and then
124 measuring maternal transmission ($1 - \mu$) to the newly emerged offspring of each subline (Figure
125 2, Table S2)[20,21]. The final dataset comprised 365 F0 females and 3,612 F1 offspring. Overall, we
126 found a significant interaction effect between the *Wolbachia*-host genotype and temperature
127 (GLMM LRT, $\chi^2_{(9)} = 23.49$, $P = 0.005$), such that temperature effects on maternal transmission
128 varied depending on the *Wolbachia*-host genotype. For most *Wolbachia*-host genotypes, mean
129 rates of maternal transmission were perfect (e.g., *w*Ri-*D. simulans*) or near-perfect (e.g., *w*Mel-
130 like *w*Seg-*D. seguyi*) and invariant across the two temperatures (Figure 2, Table S3), with the
131 exception of a few specific *Wolbachia*-host genotypes. Maternal transmission of *w*Mel by *D.*
132 *melanogaster* ($W = 251.5$, $P = 0.003$) and *w*Aura by *D. auraria* ($W = 154$, $P = 0.038$) decreased
133 significantly at 20°C; although, *w*Mel experienced a much greater decline in the average rate of
134 transmission (14.9%) than *w*Aura (2.8%). In contrast, B-group *w*Mau transmission by *D.*
135 *mauritiana* increased slightly by 3.4% in the cold at 20°C ($W = 117$, $P = 0.019$). Notably, our
136 analysis also revealed a significant effect of sex (GLMM LRT, $\chi^2_{(1)} = 63.71$, $P < 0.001$), whereby
137 rates of maternal transmission tended to be lower to female offspring than males (Table S2). This
138 finding is consistent with our previous findings for *w*Mel[21] and the *w*Mel-like *w*Yak strain in *D.*
139 *yakuba*[20], but counter to theoretical expectations that selection should favor faithful transmission
140 to female offspring[64,65].
141 To test for temperature effects on *Wolbachia* at the tissue level, we dissected out the
142 ovaries from a subset of the same F0 females assessed for maternal transmission above ($N =$
143 183). For this analysis we used qPCR to measure *Wolbachia* densities in the ovaries and the
144 remaining somatic carcass tissue (Figure 3). We found a significant interaction effect between

145 the *Wolbachia*-host genotype and temperature on *Wolbachia* density in ovaries (Two-way
146 ANOVA; $F_{(9,161)} = 4.286$, $P < 0.001$) and the remaining carcasses ($F_{(9,161)} = 10.612$, $P < 0.001$),
147 such that temperature effects on *Wolbachia* density varied depending on the *Wolbachia*-host
148 genotype. While we uncovered considerable variation depending on the *Wolbachia*-host
149 genotype and temperature, *Wolbachia* ovary densities generally tended to decline at 20°C for the
150 majority of systems (Figure 3, Table S4). Five of the *Wolbachia* strains (*w*Mel, *w*Ri, *w*Ana, *w*Ha,
151 and *w*Mau) decreased in density in the ovaries in the cold. In contrast, carcasses exhibited
152 variation in the directionality of changes in *Wolbachia* density. *w*Mel, *w*MelCS, *w*Seg, and
153 *w*Aura densities decreased significantly in the cold, whereas *w*Cha and *w*Mau significantly
154 increased. *w*Cha densities in carcasses were roughly an order of magnitude lower than all other
155 strains, regardless of temperature, suggesting a relatively high degree of localization to the
156 ovaries. *w*Mel, the strain that experienced the most dramatic decline in transmission in the cold
157 (Figure 2), was also the only *Wolbachia* strain that experienced a significant decline in
158 *Wolbachia* density in both the ovaries and the carcasses in the cold. This included a particularly
159 large decline in density in the carcasses (a 4.7-fold reduction) compared to the other strains.
160 For the three *Wolbachia*-host systems with temperature-dependent transmission (*w*Mel,
161 *w*Aura, and *w*Mau), we also tested for a correlation between transmission rates and *Wolbachia*
162 density in the ovaries and carcasses of the same individual females (Figure S1). Declining *w*Mel
163 transmission in the cold was significantly correlated with *Wolbachia* density in the ovaries
164 (Spearman's $\rho = 0.537$, $P = 0.022$), but not the carcasses ($\rho = 0.392$, $P = 0.108$), providing
165 additional support that reduced *w*Mel density in reproductive tissues contributes to transmission
166 breakdown in the cold. Maternal transmission of *w*Aura by *D. auraria* did not strongly correlate
167 with *w*Aura density in the ovaries ($\rho = -0.244$, $P = 0.380$) or the carcasses ($\rho = 0.035$, $P = 0.902$).
168 Finally, increasing maternal transmission of *w*Mau by *D. mauritiana* in the cold did not correlate
169 with *w*Mau density in the ovaries ($\rho = -0.119$, $P = 0.649$), but was significantly correlated with
170 density in the carcasses ($\rho = 0.549$, $P = 0.022$).
171 Finally, we examined how temperature impacts cellular *Wolbachia* abundance at the site
172 of germline formation in stage 10 oocytes during host oogenesis. At this stage, *w*Mel *Wolbachia*
173 localization at the posterior cortex of the oocyte is considered to be a critical step in the process
174 of germline-to-germline *Wolbachia* maternal transmission[14,15,21,36,59–63]. We imaged a total of 283
175 stage 10 oocytes from eight-day-old females reared at the two different temperatures and

176 quantified cellular *Wolbachia* abundance (measured as corrected total cell fluorescence; CTCF)
177 in the whole oocytes, the posterior region, and the posterior cortex (Figure S2)[14,15,21]. We defined
178 the posterior region as the posterior 1/8th portion of the oocyte and the posterior cortex as the
179 narrow cortical region of Vasa expression (a germline protein component)[15,63]. For the sake of
180 clarity and consistency with the literature, we refer to our *Wolbachia* quantifications with
181 confocal microscopy here as "cellular *Wolbachia* abundance" in oocytes, as opposed to the
182 quantification of "*Wolbachia* density" at the tissue level using qPCR (described above).
183 Cellular *Wolbachia* abundance in whole oocytes (Two-way ANOVA; $F_{(9,263)} = 2.9$, $P =$
184 0.003), at the posterior region ($F_{(9,263)} = 4.16$, $P < 0.001$), and at the posterior cortex ($F_{(9,263)} =$
185 2.41, $P = 0.012$) depended on significant two-way interactions between the *Wolbachia*-host
186 genotype and temperature. As with *Wolbachia* density, cellular *Wolbachia* abundance in oocytes
187 varied considerably depending on the *Wolbachia*-host genotype and temperature (Figures 4, S3).
188 The cellular abundance of six of the *Wolbachia* strains (*w*MelCS, *w*Seg, *w*Ana, *w*Aura, and *w*Tri,
189 and *w*Ha) declined significantly throughout whole oocytes in the cold (Table S5). Temperature
190 affected fewer strains (only *w*Mel, *w*MelCS, *w*Ri, and *w*Aura) at the posterior region and the
191 posterior cortex, the location of the developing germline. *w*Mel and *w*Aura, the two strains
192 transmitted at significantly lower rates in the cold, both declined significantly in abundance in
193 the posterior oocyte region ($W = 113$, $P = 0.015$; $W = 172$, $P = 0.041$). *w*Mel cellular abundance
194 also significantly declined at the posterior cortex ($W = 122$, $P = 0.002$). Interestingly, *w*MelCS
195 also exhibited a significant decline in cellular abundance in the posterior region ($W = 203$, $P <$
196 0.001) and the cortex ($W = 205$, $P < 0.001$), despite the fact that *w*MelCS transmission by *D.*
197 *melanogaster* was not altered in the cold (Figure 2). This can perhaps be explained by the fact
198 that, of all 10 strains, *w*MelCS had the highest cellular abundance at the posterior region and
199 cortex, regardless of temperature. Finally, *w*Ri was perfectly transmitted by *D. simulans* at both
200 temperatures, but *w*Ri abundance increased at the oocyte posterior region ($W = 45$, $P = 0.004$)
201 and the cortex ($W = 49$, $P = 0.008$) in the cold. Also of note, *w*Aura and *w*Tri occurred at
202 particularly low abundances in the oocyte posterior region and the posterior cortex, regardless of
203 temperature, despite both being transmitted at relatively high rates by their female hosts ($1 - \mu >$
204 0.967).
205 Our analyses revealed that the diverse *Wolbachia* strains and *Drosophila* host species
206 exhibit extensive variation in *Wolbachia* density in host tissues (Figure 3) and abundance in host

207 oocytes (Figure 4). We hypothesized that this diversity may be explained by factors in the
208 *Wolbachia* or host genomes (or both). If so, we expect closely related *Wolbachia* strains (or host
209 species) to exhibit similar patterns of *Wolbachia* localization in host tissues[15,66,67]. We used the
210 *Wolbachia* and host trees (Figure 1) to test whether patterns of *Wolbachia* localization in tissues
211 and oocytes exhibit phylogenetic signal using Pagel's λ[68]. A value of 1 is consistent with trait
212 evolution that entirely agrees with the *Wolbachia* (or host) phylogeny, suggesting factors in the
213 *Wolbachia* genome (or host) contribute to *Wolbachia* localization patterns (i.e., strong
214 phylogenetic signal). In contrast, a value of 0 is consistent with trait evolution that occurs
215 independently of phylogenetic relationships[68,69]. We found no evidence that *Wolbachia* density
216 in the ovaries and carcasses, nor cellular abundance in the oocytes, exhibit phylogenetic signal
217 on the *Wolbachia* phylogeny (Table S6, Figure S4), implying that factors in the *Wolbachia*
218 genome do not account for observed diversity. In contrast, we found that *Wolbachia* density in
219 the ovaries at 25°C exhibits strong, significant phylogenetic signal on the host phylogeny ($\lambda =$
220 1.000, $P = 0.001$), implying that factors in the host genome may help determine observed
221 diversity of *Wolbachia* densities in host ovaries. In this instance, related species in the *montium*
222 species group tended to have lower *Wolbachia* densities in the ovaries relative to the
223 *melanogaster* subgroup (see Figure S5). Divergent *D. ananassae* also had a higher *Wolbachia*
224 density than all the other host species. We also found that cellular *Wolbachia* abundance in the
225 oocyte posterior region ($\lambda = 1.000$, $P = 0.037$) and the posterior cortex ($\lambda = 1.000$, $P = 0.036$)
226 exhibited a significant signature of phylogenetic signal at 20°C on the host phylogeny. This
227 pattern is largely driven by the relatively low abundance of *Wolbachia* in the posterior oocytes of
228 the two closely related species *D. triauraria* and *auraria*.
229
230 **DISCUSSION**
231 Maternal transmission rates are a key determinant of *Wolbachia* prevalence in host
232 populations[17,55]. For many *Wolbachia* strains and host species, we found that maternal
233 transmission is generally high and stable across two ecologically relevant temperatures[21,70]. Two
234 *Wolbachia* strains (*w*Aura and B-group *w*Mau) exhibited minor temperature-dependent changes
235 in transmission, but *w*Mel stood out with a relatively large decrease in transmission as
236 temperature dropped from 25° to 20°C (Figure 2). Maternal transmission is generally expected to
237 depend on *Wolbachia* density in host reproductive tissue[20,34,43,71], and specifically within

238 developing oocytes[14,15,21,36,59–63]. Our analyses uncovered considerable, significant variation in
239 *Wolbachia* densities at the tissue level and cellular abundances in oocytes, which also often
240 varied depending on temperature. With the exception of *w*Mel, *Wolbachia* densities in ovary
241 tissue generally did not predict maternal transmission rates (Figures 3, S1). In stage 10 oocytes,
242 declines in the cellular abundance of *w*Mel and *w*Aura at the posterior region coincided with
243 declining transmission in the cold (Figure 4), but the *w*MelCS and *w*Ri strains also experienced
244 changes in cellular abundance that did not correlate with differences in maternal transmission.
245 Together, these results suggest that maternal transmission rates cannot be accurately predicted
246 from measurements of *Wolbachia* quantities in ovary tissue or late-stage oocytes. First, we
247 explore the diverse patterns of *Wolbachia* localization in relation to maternal transmission in our
248 comparative analyses. Then, we examine why maternal transmission of some strains, particularly
249 *w*Mel, may be impacted by temperature.
250 At the tissue level, we found that *Wolbachia* densities in the ovaries generally did not
251 predict rates of maternal transmission, with the exception of *w*Mel. *w*Mel density in the ovaries
252 of individual females was tightly correlated with declining transmission rates in the cold (ρ =
253 0.537, Figure S1). Temperature did not alter *w*Aura density in the ovaries despite declining
254 *w*Aura transmission in the cold, and *w*Mau density counterintuitively declined at 20°C despite
255 transmission increasing. Other strains (e.g., *w*Ri and *w*Ha in *D. simulans*) experienced large
256 declines in *Wolbachia* ovary density at 20°C with no impact on maternal transmission.
257 *Wolbachia* densities in the remaining somatic carcass tissue also generally did not predict
258 declining transmission in the cold; however, *w*Mau densities in the carcasses of individual
259 females were strongly correlated with increased transmission in the cold (ρ = 0.549; discussed
260 further below). Notably, *w*Cha was exceptional in terms of its very low density in carcass tissue
261 relative to other strains, despite perfect transmission at both temperatures.
262 At the cellular level, *Wolbachia* abundance in stage 10 oocytes may help explain why
263 *w*Mel and *w*Aura experienced declining transmission in the cold. Many strains experienced
264 declines in cellular *Wolbachia* abundance throughout the whole oocyte at 20°C (Figure 4A), but
265 this was generally unrelated to transmission rates. *w*Mel was one of the few strains that had a
266 significant reduction in cellular abundance at the posterior region (Figure 4B) and cortex (Figure
267 4C), the site of germline formation. Similarly, *w*Aura had a reduced abundance in the posterior
268 region at 20°C (but not at the cortex). *w*MelCS (closely related to *w*Mel) was the only additional

269 strain with significant reductions in abundance at the posterior region and the cortex. However,
270 *w*MelCS occurred at a much higher absolute abundance than *w*Mel, *w*Aura, and all other
271 *Wolbachia* strains, which may explain why transmission remained high at 20°C (discussed
272 further below). We conjecture that there is presumably a minimum cellular abundance required
273 for efficient transmission, and *Wolbachia* strains like *w*MelCS that are generally very abundant
274 are less likely to fall below this threshold. A reduction in cellular abundance at the oocyte
275 posterior implies that fewer *Wolbachia* cells will be incorporated into the germline later during
276 host development, perturbing germline-to-germline maternal transmission[21]. The fact that both
277 *w*Mel and *w*Aura had significantly reduced abundances in the posterior region at 20°C implies
278 that perturbations of cellular *Wolbachia* abundance in this region may help explain why some
279 *Wolbachia* strains have reduced transmission in the cold. *w*Ri was the only other *Wolbachia*
280 strain with an altered abundance at the oocyte posterior region and cortex, but cellular abundance
281 increased at 20°C. This may help explain why maternal transmission of *w*Ri remained perfect at
282 20°C. Interestingly, a low absolute abundance of *Wolbachia* was not necessarily associated with
283 declining maternal transmission. The *w*Tri strain (closely related to *w*Aura) occurred at a lower
284 posterior abundance than all other strains, despite maintaining a high rate of transmission at both
285 temperatures. It is important to note that our analysis of stage 10 oocytes is only a snapshot of
286 host development. Other unexamined stages of development, including embryogenesis, could
287 also be involved mediating maternal transmission. For instance, cool temperatures could impact
288 *Wolbachia* localization at the newly formed germline of late blastoderm and cellularized
289 embryos, which could influence maternal transmission[15,60].

290 Our comparative analysis highlights how *w*Mel seems to be especially susceptible to
291 cooling temperatures[21], which is consistent with our previous work suggesting the strain is less
292 prevalent in temperate host populations due to declining transmission in the cold[21,58]. In
293 transinfected mosquitoes, *w*Mel maternal transmission and densities are also more susceptible to
294 heat stress relative to another *Wolbachia* strain, *w*AlbB[25,26,33,34,43]. A number of factors could
295 plausibly help explain why *w*Mel maternal transmission is especially impacted by the cool
296 temperature, relative to other strains. At the tissue level, *w*Mel was the only *Wolbachia* we
297 examined that exhibited a significant decline in *Wolbachia* density in both the ovaries and the
298 carcasses at 20°C (Figure 3). Declining transmission was highly correlated with declining *w*Mel
299 density in the ovaries, plus *w*Mel stood out with a dramatic decline in *Wolbachia* density in

300 carcasses at 20°C compared to other strains. While *w*Mel is generally thought to follow a
301 germline-to-germline route of maternal transmission during oogenesis, our recent work and
302 others suggests that the strain may also rely on a soma-to germline mode of transmission[15,72,73].
303 *w*Mel *Wolbachia* are capable of cell-to-cell migration[73] and *w*Mel injected directly into the
304 abdomen of adult *D. melanogaster* females can migrate to and occupy the germline and follicle
305 stem cells[72]. The declines of *w*Mel densities throughout host tissues could potentially impact
306 routes of transmission originating in somatic tissue. At the cellular level, *w*Mel is also one of the
307 few strains (in addition to *w*Aura) to experience a decline in abundance at the posterior of stage
308 10 oocytes, which is expected to impact a germline-to-germline route of transmission. The
309 concurrent reduction in *Wolbachia* density in female tissues and oocytes may be a one-two
310 punch that impacts both soma- and germline-to-germline routes of *w*Mel transmission.
311 The juxtaposition between *w*Mel and *w*MelCS is interesting, because the two strains
312 diverged recently in only the last 3,000-14,000 years[74]. The *w*Mel and *w*MelCS strains we used
313 in our study are highly similar (0.007% third-position pairwise differences). Despite the close
314 relationship, *w*MelCS transmission was not impacted by temperature and the strain occurred at a
315 higher cellular abundance at the oocyte posterior than any of the other strains that we examined,
316 regardless of temperature. Some oocytes contained especially large quantities of *w*MelCS
317 throughout the whole oocyte and at the posterior (Figure S6), as compared to all the other
318 oocytes we examined (e.g., Figure S3). *w*MelCS is only found at low frequencies in a few
319 populations of *D. melanogaster*[74,75], which is attributed to the fact that ancestral *w*MelCS was
320 largely replaced by *w*Mel in global populations of *D. melanogaster* in roughly the last 50 to 100
321 years[76–79]. Perhaps deleterious host effects associated with a high cellular *w*MelCS abundance in
322 oocytes may have contributed to the global replacement of *w*MelCS by *w*Mel. To ensure
323 maternal transmission, *Wolbachia* cells must maintain an association with the host germline
324 without perturbing highly conserved processes of germline and oocyte development[15,62,63,80].
325 Migration of *w*Mel to the posterior germ plasm is coincident with recruitment of host factors
326 required from germline formation and anterior/posterior and dorsal/ventral axis formation[62] and
327 an excessively high *Wolbachia* abundance can disrupt dorsal/ventral axis determination[60,62,80,81].
328 Perhaps similar deleterious effects may help explain why the highly abundant *w*MelCS strain
329 was replaced by *w*Mel, despite a higher rate of transmission in the cold. Pervious works has also
330 shown that higher densities of *w*MelCS in *D. melanogaster* often covaries with a reduced

331 lifespan[75]. Of course, we cannot rule out the possibility that the host genome also contributes to
332 some of the differences we observed here between *w*MelCS and *w*Mel[20,21]. Indeed, our
333 phylogenetic analyses suggest the host genome is an important determinant of *Wolbachia*
334 abundance in oocytes (Table S6).

335 The divergent B-group *w*Mau strain was the only strain where transmission significantly
336 increased at 20°C (Figure 2). Transmission was high at 25°C and increased to perfect at 20°C.
337 Our previous work suggests the *w*Mau strain may also be an outlier in its mode of transmission
338 during oogenesis relative to A-group *Wolbachia*, which tend to exhibit evidence of a germline-
339 to-germline route of transmission[15]. *w*Mau occurs at relatively low abundance at the posterior
340 cortex of stage 10 oocytes (Figure 4), but *w*Mau cells are frequently found within the somatically
341 derived follicle cells surrounding the oocytes (Figure S6)[15], which is consistent with a soma-to-
342 germline route of transmission. The presence of *Wolbachia* in the follicle cells is generally not
343 the case for A-group *Wolbachia* (with the exception of *w*Mel, discussed above). We found that
344 *w*Mau was also one of the few strains (in addition to *w*Cha) where *Wolbachia* density in the
345 somatic carcass tissues significantly increased at 20°C (Figure 3), which may help explain why
346 transmission increased slightly at 20°C. *w*Mau transmission was also strongly correlated with
347 *Wolbachia* densities in the carcasses of individual females. Notably, our previous analysis of two
348 other *w*Mau-*D. mauritiana* genotypes using three- to five-day old females found perfect rates of
349 transmission at 25°C[40], unlike our results here (Figure 2). This suggests that differences in fly
350 age[82], the *Wolbachia* and host genomes[21], or other unknown factors may also contribute to
351 variation in rates of maternal transmission.

352 The *w*Mau findings also may inform our previous work on the thermoregulatory behavior of
353 *Drosophila* host species. We found that *Drosophila* species carrying A-group *Wolbachia*,
354 including *w*Ri and *w*Ha, tend to prefer cooler temperatures on a thermogradient (relative to flies
355 without *Wolbachia*), whereas *D. mauritiana* flies carrying *w*Mau prefer warmer temperatures[66].
356 Taken together, these results suggest that fly movement to cool temperatures reduces the density
357 of A-group *Wolbachia* in host tissues, whereas movement to warm temperatures reduces B-
358 group *w*Mau density. This is consistent with the inference that flies may thermoregulate as a
359 behavioral response to ameliorate negative effects of infection and a high *Wolbachia* density[67,83–
360 86]. Movement to cooler temperatures with A-group *Wolbachia* (i.e., behavioral chill) and to
361 warmer temperatures with B-group *w*Mau (behavioral fever) are both behaviors that would

362 reduce *Wolbachia* density in host tissues according to our results here (Figure 3). This finding
363 motives further work dissecting the relationships among thermoregulatory behavior, *Wolbachia*
364 density in host tissues, and maternal transmission.

365 Our phylogenomic analyses revealed that *Wolbachia* density in the ovaries at 25°C and
366 cellular *Wolbachia* abundance in the oocyte posterior region and cortex at 20°C all exhibit
367 phylogenetic signal on the host phylogeny (Table S6, Figure S5), implying that factors in the
368 host genome help explain the observed diversity in *Wolbachia* localization across species. For
369 example, interspecific variation in the host proteins that *Wolbachia* engage during oogenesis
370 could plausibly influence *Wolbachia* localization patterns at the posterior cortex in stage 10
371 oocytes[15]. Unfortunately, it is not yet known how *Wolbachia* engage host factors like kinesin
372 during oogenesis[63]. Other work also suggests the host genome can influence *Wolbachia*
373 abundance in oocytes[21] and embryos[60]. Similarly, genome-wide screens reveal that host factors
374 play an important role in determining cellular *Wolbachia* abundance[87,88]. The findings here
375 complement our previous comparative analyses that suggest the *Wolbachia* genome also
376 contributes to variation in *Wolbachia* localization patterns in oocytes[15] and effects on host
377 thermoregulatory behavior[66]. While we did not identify any traits that exhibit phylogenetic signal
378 on the *Wolbachia* phylogeny, it is worth noting that relatively few *Wolbachia* genomic changes
379 (e.g., in the ampliconic "Octomom" gene region) are required to influence density and tissue
380 distributions[75,89–92]. This highlights the potential for rapid changes in these traits and their effects
381 on transmission.

382 The rate of *Wolbachia* maternal transmission, in conjunction with *Wolbachia* effects on host
383 fitness and cytoplasmic compatibility (CI), ultimately determine *Wolbachia* prevalence in host
384 populations[17,55]. In this study, we uncovered limited variation in maternal transmission rates
385 across temperatures, despite dramatic variation in *Wolbachia* localization patterns within host
386 tissues. Nonetheless, a few *Wolbachia* strains, particularly *w*Mel, had variable transmission rates
387 that are likely to impact *Wolbachia* prevalence in natural host populations. For instance *w*Mel
388 causes weak CI[82,93,94] and occurs at lower frequencies globally in temperature host populations,
389 which can plausibly be explained by declining transmission in the cold (Figure 2)[21]. Similarly,
390 *w*Mau does not cause CI and occurs at intermediate frequencies in *D. mauritiana* on
391 Mauritius[40,95]. Our results suggest temperature-related variation in *w*Mau transmission may
392 perhaps help contribute to intermediate frequencies. In contrast, *Wolbachia* strains like *w*Ri[17–

393 [19,96], *w*Ha[97–99], and *w*Ana[100,101] cause strong CI and tend to occur at high equilibrium frequencies
394 in nature. In addition to strong CI, our results suggest that stable transmission rates may help
395 these strains maintain high frequencies in the face of fluctuating conditions (Figure 2). However,
396 this may not always be the case, as we found that maternal transmission the strong CI-causing
397 strain *w*Aura[51,100] can be perturbed by temperature. Unlike CI and *Wolbachia* maternal
398 transmission, the role of *Wolbachia* effects on host fitness in natural *Drosophila* populations is
399 poorly understood, although recent work suggests *Wolbachia* block viruses in their native
400 *Drosophila* hosts[8,9,102,103].
401 Understanding how temperature influences *Wolbachia* maternal transmission, especially in
402 relation to other key factors like CI and host fitness effects, is critical for explaining global
403 *Wolbachia* prevalence in host populations. Research on this front will also inform *Wolbachia*-
404 based biocontrol programs, as thermally stable *Wolbachia* strains can be leveraged to improve
405 the efficacy of *Wolbachia*-based biocontrol applications in mosquito populations that experience
406 extreme environments[25,104]. In this respect, temperature and the environment are emerging as key
407 factors that mediate interactions between *Wolbachia*, their hosts, and pathogens.
408
409 **METHODS**
410 *Fly lines*
411 We evaluated 10 different *Wolbachia* strains that naturally occur in eight different
412 *Drosophila* species (Table S1). For two of these host species, we tested multiple *Wolbachia*-host
413 genotypes: *w*Mel and *w*MelCS in *D. melanogaster* and *w*Ri and *w*Ha in *D. simulans*. With the
414 exception of the *w*MelCS-*D. melanogaster* line, all the *Wolbachia*-host genotypes were sampled
415 from nature to form isofemale lines, such that single gravid females were collected from the field
416 and placed individually into vials (see [66] for further discussion of the *w*MelCS genotype). For the
417 maternal transmission experiments explained below, we paired each *Wolbachia*-positive female
418 with *Wolbachia*-free males of the same host species (Table S1). Here, we used males from
419 naturally *Wolbachia*-free isofemale lines whenever possible; however, in some cases, we were
420 unable to obtain natural genotypes without *Wolbachia*. For these species, *Wolbachia*-free
421 genotypes were created by treating the *Wolbachia*-positive genotype with 0.03% tetracycline for
422 at least four generations. After the fourth generation, we used quantitative PCR (qPCR) to
423 confirm that flies were cleared of *Wolbachia*[66]. We then reconstituted the gut microbiome of the

424 tetracycline-cleared flies by rearing them on food where *Wolbachia*-positive males of the same
425 genotype had been fed and defecated for the prior 48 hours. Tetracycline-cleared flies were given
426 at least three more generations before we conducted experiments to avoid detrimental effect of
427 the antibiotic treatment on mitochondrial function[105].
428
429 *Maternal transmission*
430 We tested how temperature influences maternal transmission and *Wolbachia* distributions
431 in host tissues by rearing females of each genotype at a moderate (25°C) and low (20°C)
432 temperatures. Prior to experiments, the isofemale lines were reared for at least two generations in
433 incubators set to each temperature and a 12L:12D light cycle (Percival Model I-36LL) on a
434 standard food diet[66]. We estimated maternal transmission at each temperature by aspirating
435 individual virgin females into vials with two 3-5 day old virgin males of the *Wolbachia*-free
436 genotype and then allowing females to lay eggs for eight days[20,21]. We crossed *Wolbachia*-
437 positive females to males without *Wolbachia*, because in crosses with *Wolbachia*-positive males,
438 *Wolbachia*-free ova produced by *Wolbachia*-positive females could be lost if they are susceptible
439 to cytoplasmic incompatibility, potentially leading to an overestimation of maternal
440 transmission[18]. The males in our experiments were all collected from the *Wolbachia*-free
441 genotypes that were maintained at 25°C.
442 Newly emerged adult F1 offspring were immediately preserved in 95% ethanol and
443 stored at -20°C for later analysis of *Wolbachia* status. For each subline, we measured maternal
444 transmission by screening five female and five male F1s for *Wolbachia* using PCR. We extracted
445 DNA from individual F1s using 96-well plates and a "squish" extraction buffer (10 mL Tris-HCl
446 [1M], 0.0372 g EDTA, 0.1461 g NaCl, 90 mL dH20, followed by 150 mL Proteinase K after
447 autoclaving) that allows for high-throughput and cost-effective DNA extraction. We screened
448 each F1 for *Wolbachia* status using previously described PCR primers for the *Wolbachia* surface
449 protein (*wsp*) and a second set of primers for the arthropod-specific 28S rDNA that served as a
450 positive control[20,40,106].
451 All statistical analyses were performed in R[107]. We computed maternal transmission for
452 each genotype at each temperature as the mean proportion of *Wolbachia*-positive offspring
453 produced by *Wolbachia*-positive mothers in each subline. We then estimated 95% bias-corrected
454 and accelerated bootstrap (BC_a) confidence intervals using the "boot.ci" function and 5000

455 iterations in the *boot* package in R[108]. We analyzed whether maternal transmission rates vary by
456 *Wolbachia*-host genotype (e.g., *w*Mel-*D. melanogaster*) and temperature using a generalized
457 linear mixed model (GLMM) logistic regression with the "glmer" function in the *lme4* R
458 package[109]. We treated the *Wolbachia* status of F1s as the dependent variable and then included
459 sex, the *Wolbachia*-host genotype, temperature, and a two-way interaction between the
460 *Wolbachia*-host genotype and temperature as independent variables. We included sex in the
461 model because we previously found that *w*Mel-like *Wolbachia* (*w*Mel and *w*Yak) are transmitted
462 more efficiently to male offspring[20,21]. Finally, we included the subline of each F1 as a random
463 effect. We assessed significance of the fixed effects with a likelihood ratio test (LRT) and type
464 III sum of squares using the "mixed" function in the *afex* package[110]. Lastly, we used Wilcoxon
465 rank-sum tests to evaluate whether transmission rates differ between 25° and 20°C for each
466 strain.
467
468 *Wolbachia density in host ovaries*
469 After each female was allowed to lay for eight days, we immediately dissected out her
470 ovaries in chilled 1X PBS. Both the ovaries and remaining carcass were then frozen at -80°C.
471 We then used qPCR to quantify *Wolbachia* density in the dissected ovaries and carcasses of each
472 individual female. DNA was first extracted using a DNeasy Blood and Tissue Kit (Qiagen) and
473 then amplified the *Wolbachia*-specific locus *ftsZ* and the *Drosophila*-specific locus *nAcRalpha-*
474 *34E*. Preliminary analyses indicated that separate primers were needed for *Wolbachia* in the
475 divergent A-Group (F: 5'-ATCCTTAACTGCGGCTCTTG-3', R: 5'-
476 TTCATCACAGCAGGAATGGG-3') and B-Group lineages (F: 5'-
477 CAGAGAAGCAAGAGCGGTAG-3', R: 5'-TCTTCAAGTCCAAGCTCTGC -3'). We were
478 able to use a single set of primers for all the *Drosophila* hosts (F: 5'-
479 CTATGGTCGTTGACAGACT-3', R: 5'-GTAGTACAGCTATTG TGGC-3'). We generated
480 efficiency curves to confirm that each primer pair amplified with adequate efficiency for each
481 *Wolbachia* strain and host species. All qPCR reactions were amplified using the following
482 cycling conditions: 50°C for 2 min, 95°C for 2 min, and then 40 cycles, with one cycle
483 consisting of 95°C for 15 s, 58°C for 15 s, and 72°C for 1 min. We used the average cycle
484 threshold (Ct) value of three technical replicates for each sample. We then estimated relative
485 *Wolbachia* density as $2^{\Delta Ct}$, where $\Delta Ct = Ct_{nAcRalpha-34E} - Ct_{ftsZ}$[111]. We used a two-way

486 ANOVA and type III sums of squares to test whether log-transformed *Wolbachia* density varied
487 among *Wolbachia*-host genotypes and temperature for both the ovaries and the carcasses. We
488 also used Wilcoxon rank-sum tests to test whether densities differed between 25° and 20°C for
489 each tissue and *Wolbachia*-host genotype.
490
491 *Cellular Wolbachia abundance in host oocytes*
492 We used previously described protocols and confocal imaging to quantify cellular
493 *Wolbachia* in host oocytes at each temperature[15,21]. Briefly, we paired 20 newly emerged virgin
494 *Wolbachia*-positive females *en masse* with ten 3-5 day old virgin *Wolbachia*-negative males in
495 individual vials for eight days to stimulate oocyte production. Females were then separated using
496 CO_2 and ovaries were dissected in a chilled dish of 1X PBS. Ovaries were fixed in 200 µl of
497 devitellinizing solution (2% paraformaldehyde and 0.5% v/v NP40 in 1X PBS) mixed with 600
498 µl of heptane for 20 min on a shaker at room temperature. We then removed the organic layer
499 using a brief centrifugation and washed the ovaries three times with PBS-T (0.1% Triton X-100
500 in 1X PBS), followed by three additional five min washes. Samples were treated with RNAse A
501 (10 mg/ml) and left overnight at room temperature. The samples were then washed in PBS-T
502 multiple times over two hours and then stained with a dilute solution of Alexa 488 phalloidin on
503 a shaker for two hours for actin staining. Subsequently, the samples were washed again multiple
504 times over the course of two more hour. Finally, the wash solution was removed and we added
505 60 µl of propidium iodide (PI) in mounting media (VECTASHIELD) and left again overnight.
506 Ovaries were then mounted and carefully separated out again for ease of imaging. Slides were
507 sealed with a coat of nail polish and stored at -20°C until imaging.
508 We used a Zeiss Olympia confocal microscope and the 40x Plan-Apochromat oil
509 objective for image acquisition. Alexa 488 was imaged using the 488 nm laser line and emissions
510 were collected from 493 to 584 nm. Propidium iodide was imaged using the 488 and 561 nm
511 lines and emissions were collected from 584 to 718 nm. Stage 10 oocytes were identified based
512 on two criterion. First, the egg chamber had to have two compartments, one with nurse cells and
513 the other with the developing oocyte. Second, the oocyte had to account for approximately 50%
514 of the egg chamber. The top and bottom of the oocyte were identified by scanning through the
515 egg chamber and then a 0.8 µm slice was taken around the midplane. The pixel dwell time was
516 8.19 µsec.

517 Image analysis was conducted in the program Fiji[112] following Russell *et al.*[63]. We first
518 manually adjusted the contrast of each image to increase the threshold so that only white puncta
519 corresponding to *Wolbachia* cells inside the oocyte were retained and all background noise was
520 rendered black. We then used the polygon selection tool to select three different regions of the
521 oocyte (see Figure S1 in Russell *et al.*): the whole oocyte, the posterior region, and the posterior
522 cortex. We defined the posterior region as the posterior 1/8th of the oocyte and the posterior
523 cortex as the narrow cortical region where the pole plasm component Vasa is expressed[15,63]. The
524 "area" and "integrated density" were measured for each region. Additionally, the average of a
525 quadruplicate measure of "mean gray value" in background selections was measured to account
526 for any remaining background fluorescence. The corrected total cell fluorescence (CTCF) was
527 calculated as integrated density – (area x background mean gray value) for each region. We used
528 two-way ANOVAs and type III sums of squares to test whether log-transformed CTCF values
529 differed among *Wolbachia*-host genotypes and temperature in each region of the oocyte (whole
530 oocyte, posterior region, and posterior cortex). We also used Wilcoxon rank-sum tests to test
531 whether CTCF values differed between 25° and 20°C for each oocyte regions and *Wolbachia*-
532 host genotype.
533
534 *Phylogenomic analyses*
535 We conducted phylogenomic analyses to characterize the evolutionary relationships
536 among *Wolbachia* strains and *Drosophila* host species. We obtained *Wolbachia* sequences from
537 publicly available genome assemblies for *w*Mel[21], *w*MelCS[66], *w*Seg, *w*Cha[15], *w*Ri[113], *w*Ana[114],
538 *w*Aura, *w*Tri[51], *w*Ha[115], and *w*Mau[40]. We used Prokka 1.11 to identify homologs to known
539 bacterial genes in the assemblies[116]. We avoided pseudogenes and paralogs in our phylogenetic
540 analyses by selecting only single copy genes that uniquely matched a bacterial reference gene
541 identified by Prokka. We removed loci with indels by requiring all homologs to have identical
542 length in all *Wolbachia* genomes. A total of 170 full length single copy genes met these criteria,
543 totaling 135,105 bp. We then estimated a Bayesian phylogram using RevBayes 1.0.8 under the
544 GTR + Γ + I model partitioned by codon position[117]. Four independent runs were performed,
545 which all converged on the same topology. All nodes were supported with Bayesian posterior
546 probabilities >0.99.

547 We used similar methods to generate a phylogram for the *Drosophila* host species.
548 Publicly available sequences were obtained for *D. melanogaster*[118], *D. simulans*[119], *D.*
549 *mauritiana*[40], *D. seguyi*, *D. chauvacae*[120], *D. auraria*, *D. triauraria*[51], and *D. ananassae*[121]. A
550 host phylogeny was generated using the same nuclear genes implemented in Turelli *et al.*[51]:
551 *aconitase, aldolase, bicoid, ebony, enolase, esc, g6pdh, glyp, glys, ninaE, pepck, pgi, pgm, pic,*
552 *ptc, tpi, transaldolase, white, wingless,* and *yellow*. We used BLAST with the *D. melanogaster*
553 coding sequences to extract orthologs from the genomes of each host species. Sequences were
554 then aligned with MAFFT 7[122]. Finally, we used RevBayes and the GTR + Γ + I model
555 partitioned by codon position and gene to accommodate potential variation in the substitution
556 process among genes. All nodes were supported with Bayesian posterior probabilities of 1.
557 The resulting phylograms were used to test whether *Wolbachia* density and oocyte
558 cellular abundance exhibit phylogenetic signal on either the *Wolbachia* or host phylogenies. For
559 the host phylogeny, we pooled estimates of *Wolbachia* density and oocyte abundance by host
560 species, because two of the hosts (*D. melanogaster* and *D. simulans*) had data for multiple
561 genotypes carrying different *Wolbachia* strains. We used our estimates of *Wolbachia* density
562 ($2^{\Delta Ct}$) and cellular oocyte abundance (log-transformed CTCF) to test for phylogenetic signal
563 using Pagel's lambda (λ)[68]. A Pagel's λ of 0 indicates that character evolution occurs
564 independently of phylogenetic relationships, whereas λ = 1 is consistent with a Brownian motion
565 model of character evolution. We used the "phylosig" function and a likelihood ratio test (LRT)
566 in the *phytools* package[123] to compare the fitted value to a model assuming no phylogenetic
567 signal (λ = 0). We also used a Monte Carlo-based method to generate 95% confidence intervals
568 surrounding our estimates using 1,000 bootstrap replicates in the *pmc* package[124].
569

570 **ACKNOWLEDGEMENTS**

571 We are especially thankful to W. Sullivan for very useful discussions that improved the
572 quality of this manuscript. We thank W. Conner for assistance with bioinformatic analyses. J.
573 Statz provided thoughtful feedback on the manuscript. We thank the Genomics Core, the
574 Environmental Control for Organismal Research (ECOR) facility, and the Center for
575 Biomolecular Structure and Dynamics at the University of Montana. This study was funded
576 by National Science Foundation CAREER (2145195) and National Institute of General Medical
577 Sciences of the National Institutes of Health MIRA (R35GM124701) awards to B.S.C.

AUTHOR CONTRIBUTIONS

M.T.J.H. designed the project, collected data, performed analyses, and prepared the manuscript. T.B.W. collected data. B.S.C. acquired funding, designed the project, prepared the manuscript, and provided leadership. All authors reviewed and edited the manuscript prior to submission.

COMEPETING INTERESTS

The authors declare no competing interests.

DATA AVAILABILITY

All newly generated data will be made publicly available upon publication.

591 **FIGURES**

592 **Figure 1. Divergent *Wolbachia* strains found in *Drosophila* host species. (A)** Estimated
593 Bayesian phylogram of the 10 A- and B-group *Wolbachia* strains included in the study. The
594 phylogram was estimated using 170 single-copy genes of identical length in all genomes,
595 spanning 135,105 bp. **(B)** Estimated Bayesian phylogram of the eight *Drosophila* species using
596 20 single-copy genes. All nodes on both trees are supported with Bayesian posterior probabilities
597 of 1. Estimates of *Wolbachia* and *Drosophila* divergence reported in millions of years ago
598 (MYA) are reproduced from Meany *et al.*[40] and Suvorov *et al.*[125], respectively. The *Wolbachia*
599 and host trees are generally discordant, as expected with frequent *Wolbachia* host
600 switching[47,48,51,53,54].

601

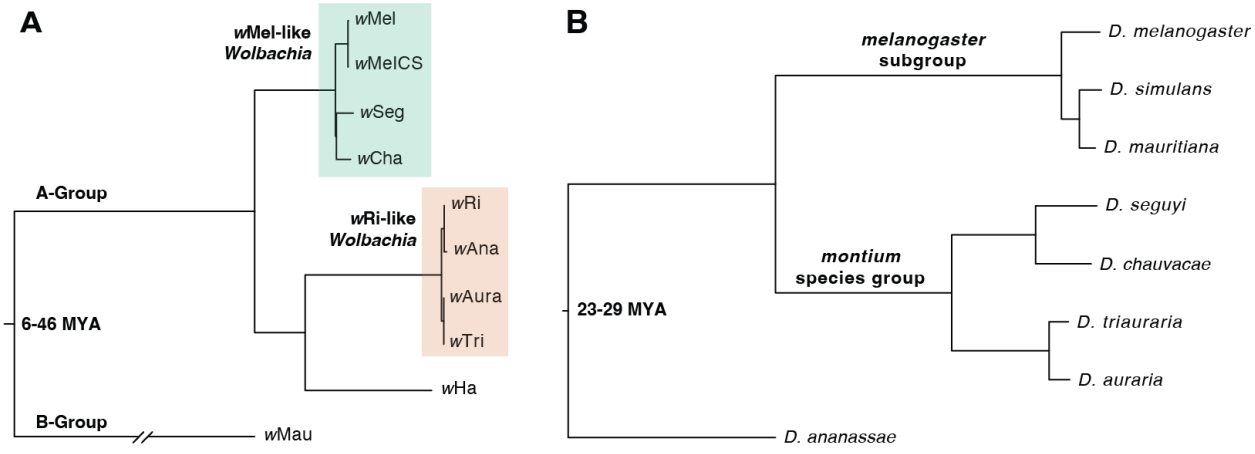

602

603 **Figure 2. Maternal transmission is high and stable across temperatures for many**
604 ***Wolbachia* strains.** Mean maternal transmission rates (±BC_a confidence intervals) of different
605 *Wolbachia* strains in their naturally associated host species. Asterisks indicate the rates of
606 maternal transmission differ between 25° and 20°C for a given *Wolbachia* strain according to a
607 Wilcoxon rank-sum test at $P < 0.05$. Below, the cladogram depicts evolutionary relationships
608 among *Wolbachia* strains.
609

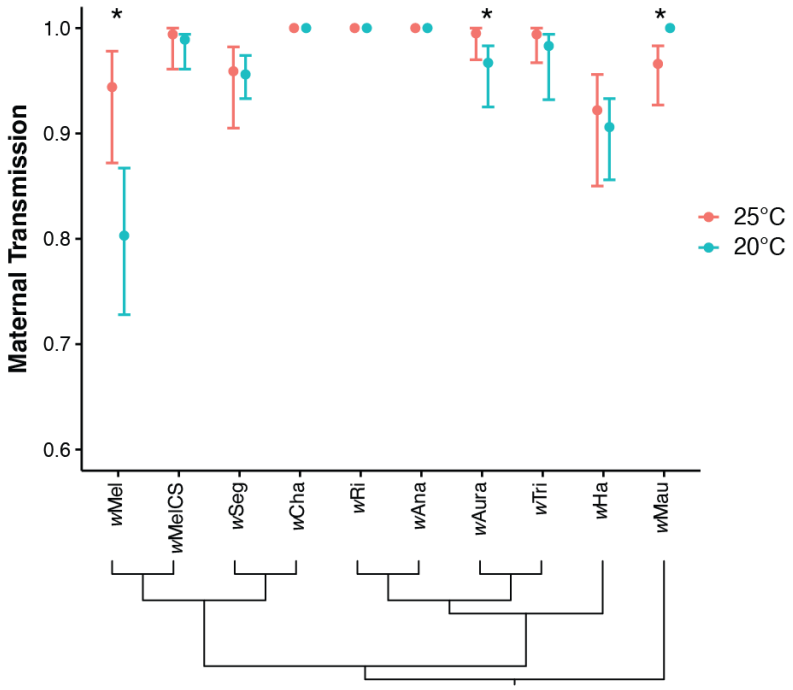

610

611 **Figure 3. *Wolbachia* densities in host tissues vary by *Wolbachia*-host system and**
612 **temperature.** *Wolbachia* densities are shown for dissected female ovaries and the remaining
613 somatic carcass tissue. Asterisks indicate the *Wolbachia* density differs between 25° and 20°C
614 for a given *Wolbachia* strain according to a Wilcoxon rank-sum test at $P < 0.05$.
615

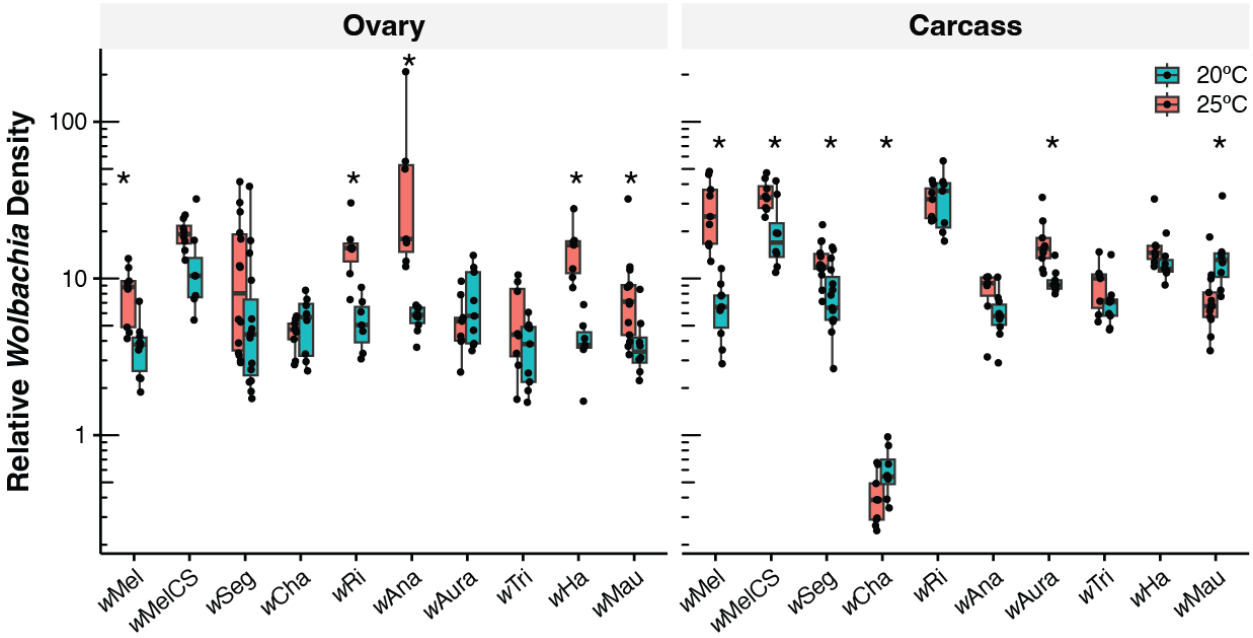

616

617 **Figure 4. Cellular *Wolbachia* abundance in late-stage oocytes generally does not align with maternal transmission rates.**
618 Cellular *Wolbachia* abundance in stage 10 oocytes (measured as fluorescence due to propidium iodide; CTCF), measured in **(A)** the
619 whole oocyte, **(B)** the posterior region, and **(C)** the posterior cortex. Asterisks indicate that *Wolbachia* abundance differs between 25°
620 and 20°C for a given *Wolbachia* strain according to a Wilcoxon rank-sum test at $P < 0.05$. **(D)** Representative confocal images of
621 *Wolbachia* strains that have decreased abundance at the posterior cortex in the cold (*w*Mel), increased abundance at the cortex in the
622 cold (*w*Ri), and no change in the cold (*w*Cha). Confocal micrographs are DNA-stained with PI (red) and actin-stained with phalloidin
623 (green). The second column depicts a single channel image of the PI stain and the third column depicts an enlarged PI-stained image
624 at the posterior cortex of each oocyte. Scale bars are set to 25 µm.
625

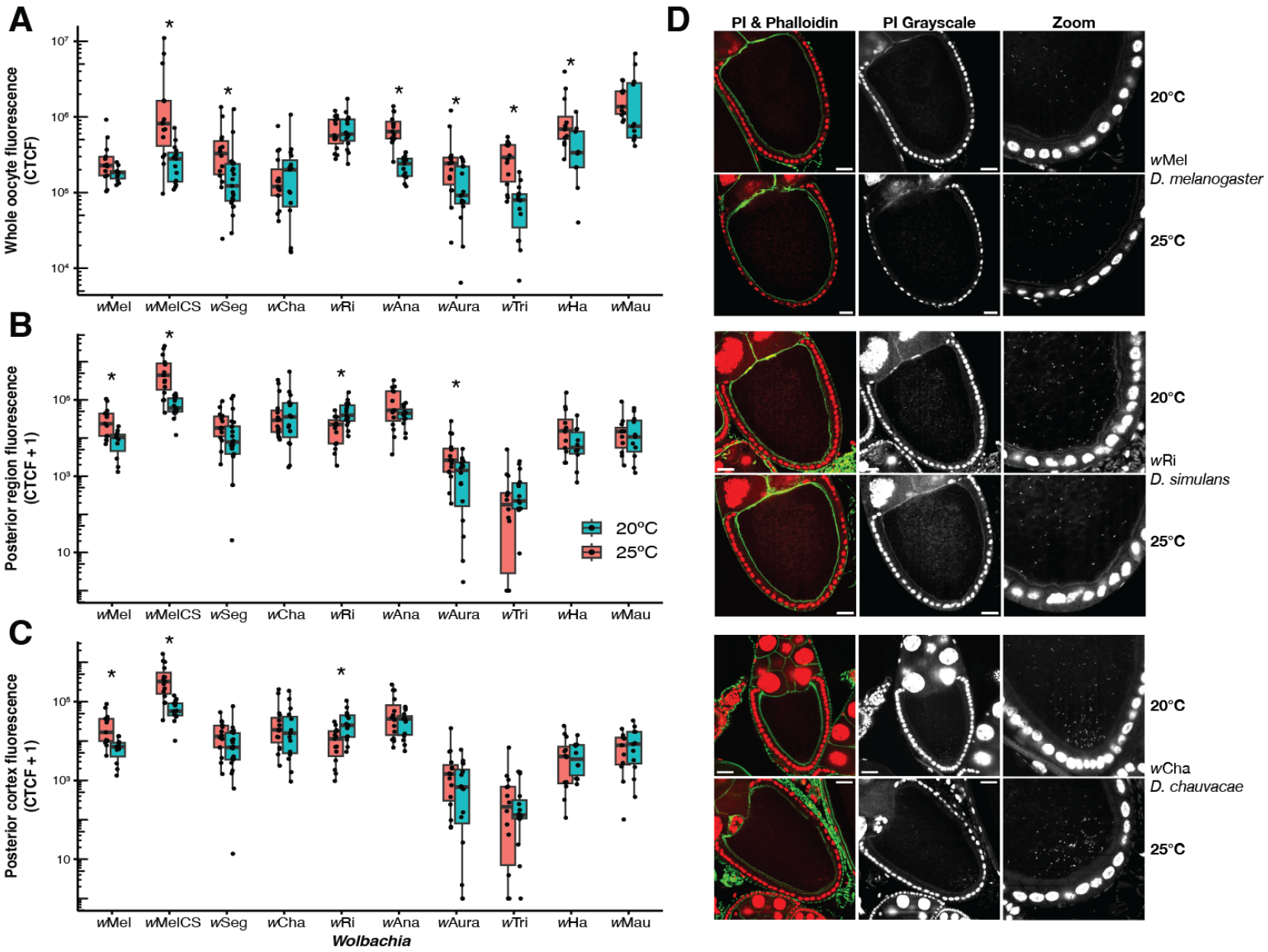
A
Whole oocyte fluorescence (CTCF)
B
Posterior region fluorescence (CTCF + 1)
C
Posterior cortex fluorescence (CTCF + 1)
wMel
wMelCS
wSeg
wCha
wRi
wAna
wAura
wTri
wHa
wMau
Wolbachia
20°C
25°C
D
PI & Phalloidin
PI Grayscale
Zoom
20°C
wMel
D. melanogaster
25°C
20°C
wRi
D. simulans
25°C
20°C
wCha
D. chauvacae
25°C

626

627 **REFERENCES**

628 1. Sudakaran, S., Kost, C. & Kaltenpoth, M. Symbiont acquisition and replacement as a
629 source of ecological innovation. *Trends Microbiol.* **25**, 375–390 (2017).

630 2. McCutcheon, J. P., Boyd, B. M. & Dale, C. The life of an insect endosymbiont from the
631 cradle to the grave. *Curr. Biol.* **29**, R485–R495 (2019).

632 3. McCutcheon, J. P. The genomics and cell biology of host-beneficial intracellular infections.
633 *Annu. Rev. Cell Dev. Biol.* **37**, 115–142 (2021).

634 4. Werren, J. H., Baldo, L. & Clark, M. E. *Wolbachia:* master manipulators of invertebrate
635 biology. *Nat. Rev. Microbiol.* **6**, 741–751 (2008).

636 5. Shropshire, J. D., Leigh, B. & Bordenstein, S. R. Symbiont-mediated cytoplasmic
637 incompatibility: what have we learned in 50 years? *Elife* **9**, e61989 (2020).

638 6. Oliver, K. M., Russell, J. A., Moran, N. A. & Hunter, M. S. Facultative bacterial symbionts
639 in aphids confer resistance to parasitic wasps. *Proc. Natl. Acad. Sci.* **100**, 1803–1807
640 (2003).

641 7. Jaenike, J., Unckless, R., Cockburn, S. N., Boelio, L. M. & Perlman, S. J. Adaptation via
642 symbiosis: recent spread of a *Drosophila* defensive symbiont. *Science* **329**, 212–215
643 (2010).

644 8. Cogni, R., Ding, S. D., Pimentel, A. C., Day, J. P. & Jiggins, F. M. *Wolbachia* reduces virus
645 infection in a natural population of *Drosophila*. *Commun. Biol.* **4**, 1–7 (2021).

646 9. Bruner-Montero, G. & Jiggins, F. M. *Wolbachia* protects *Drosophila melanogaster* against
647 two naturally occurring and virulent viral pathogens. *Sci. Rep.* **13**, 8518 (2023).

648 10. Baumann, P. Biology of bacteriocyte-associated endosymbionts of plant sap-sucking
649 insects. *Annu. Rev. Microbiol.* **59**, 155–189 (2005).

650 11. Moran, N. A., McCutcheon, J. P. & Nakabachi, A. Genomics and evolution of heritable
651 bacterial symbionts. *Annu. Rev. Genet.* **42**, 165–190 (2008).

652 12. Douglas, A. E. The microbial dimension in insect nutritional ecology. *Funct. Ecol.* **23**, 38–
653 47 (2009).

654 13. Fisher, R. M., Henry, L. M., Cornwallis, C. K., Kiers, E. T. & West, S. A. The evolution of
655 host-symbiont dependence. *Nat. Commun.* **8**, 1–8 (2017).

656 14. Russell, S. L., Chappell, L. & Sullivan, W. A symbiont's guide to the germline. *Curr. Top.*
657 *Dev. Biol.* **135**, 315–351 (2019).

658 15. Radousky, Y. A. *et al.* Distinct *Wolbachia* localization patterns in oocytes of diverse host
659 species reveal multiple strategies of maternal transmission. *Genetics* **224**, (2023).

660 16. Dunbar, H. E., Wilson, A. C., Ferguson, N. R. & Moran, N. A. Aphid thermal tolerance is
661 governed by a point mutation in bacterial symbionts. *PLoS Biol.* **5**, (2007).

662 17. Hoffmann, A. A., Turelli, M. & Harshman, L. G. Factors affecting the distribution of
663 cytoplasmic incompatibility in *Drosophila simulans*. *Genetics* **126**, 933–948 (1990).

664 18. Turelli, M. & Hoffmann, A. A. Cytoplasmic incompatibility in *Drosophila simulans*:
665 dynamics and parameter estimates from natural populations. *Genetics* **140**, 1319–1338
666 (1995).

667 19. Carrington, L. B., Lipkowitz, J. R., Hoffmann, A. A. & Turelli, M. A re-examination of
668 *Wolbachia*-induced cytoplasmic incompatibility in California *Drosophila simulans*. *PLoS*
669 *One* **6**, e22565 (2011).

670 20. Hague, M. T., Mavengere, H., Matute, D. R. & Cooper, B. S. Environmental and genetic
671 contributions to imperfect *w*Mel-like *Wolbachia* transmission and frequency variation.
672 *Genetics* **215**, 1117–1132 (2020).

673 21. Hague, M. T. J. *et al.* Temperature effects on cellular host-microbe interactions explain
674 continent-wide endosymbiont prevalence. *Curr. Biol.* **32**, 878-888.e8 (2022).

675 22. Wade, M. J. The co-evolutionary genetics of ecological communities. *Nat. Rev. Genet.* **8**,
676 185–195 (2007).

677 23. Weeks, A. R., Turelli, M., Harcombe, W. R., Reynolds, K. T. & Hoffmann, A. A. From
678 parasite to mutualist: Rapid evolution of *Wolbachia* in natural populations of *Drosophila*.
679 *PLoS Biol.* **5**, e114 (2007).

680 24. Ross, P. A., Turelli, M. & Hoffmann, A. A. Evolutionary ecology of *Wolbachia* releases for
681 disease control. *Annu. Rev. Genet.* **53**, (2019).

682 25. Ross, P. A. *et al.* Developing *Wolbachia*-based disease interventions for an extreme
683 environment. *PLoS Pathog.* **19**, e1011117 (2023).

684 26. Hien, N. T. *et al.* Environmental factors influence the local establishment of *Wolbachia* in
685 *Aedes aegypti* mosquitoes in two small communities in central Vietnam. *Gates Open Res.* **5**,
686 (2021).

687 27. Nikolouli, K. *et al.* Sterile insect technique and *Wolbachia* symbiosis as potential tools for
688 the control of the invasive species *Drosophila suzukii*. *J. Pest Sci.* **91**, 489–503 (2018).

689 28. Gong, J.-T. *et al.* Stable introduction of plant-virus-inhibiting *Wolbachia* into planthoppers
690 for rice protection. *Curr. Biol.* **30**, 4837–4845 (2020).

691 29. McMeniman, C. J. *et al.* Stable introduction of a life-shortening *Wolbachia* infection into
692 the mosquito *Aedes aegypti*. *Science* **323**, 141–144 (2009).

693 30. Hoffmann, A. A. *et al.* Successful establishment of *Wolbachia* in *Aedes* populations to
694 suppress dengue transmission. *Nature* **476**, 454–457 (2011).

695 31. Walker, T. *et al.* The *w*Mel *Wolbachia* strain blocks dengue and invades caged *Aedes*
696 *aegypti* populations. *Nature* **476**, 450–453 (2011).

697 32. Utarini, A. *et al.* Efficacy of *Wolbachia*-infected mosquito deployments for the control of
698 dengue. *N. Engl. J. Med.* **384**, 2177–2186 (2021).

699 33. Ross, P. A. *et al. Wolbachia* infections in *Aedes aegypti* differ markedly in their response to
700 cyclical heat stress. *PLOS Pathog.* **13**, e1006006 (2017).

701 34. Ross, P. A., Ritchie, S. A., Axford, J. K. & Hoffmann, A. A. Loss of cytoplasmic
702 incompatibility in *Wolbachia*-infected *Aedes aegypti* under field conditions. *PLoS Negl.*
703 *Trop. Dis.* **13**, e0007357 (2019).

704 35. Funkhouser-Jones, L. J., van Opstal, E. J., Sharma, A. & Bordenstein, S. R. The maternal
705 effect gene Wds controls *Wolbachia* titer in *Nasonia*. *Curr. Biol.* **28**, 1692–1702 (2018).

706 36. Porter, J. & Sullivan, W. The cellular lives of *Wolbachia*. *Nat. Rev. Microbiol.* 1–17 (2023).

707 37. Bright, M. & Bulgheresi, S. A complex journey: transmission of microbial symbionts. *Nat.*
708 *Rev. Microbiol.* **8**, 218–230 (2010).

709 38. Landmann, F. *et al.* Both asymmetric mitotic segregation and cell-to-cell invasion are
710 required for stable germline transmission of *Wolbachia* in filarial nematodes. *Biol. Open* **1**,
711 536–547 (2012).

712 39. Correa, C. C. & Ballard, J. *Wolbachia* associations with insects: winning or losing against a
713 master manipulator. *Front. Ecol. Evol.* **3**, 153 (2016).

714 40. Meany, M. K. *et al.* Loss of cytoplasmic incompatibility and minimal fecundity effects
715 explain relatively low *Wolbachia* frequencies in *Drosophila mauritiana*. *Evolution* **73**,
716 1278–1295 (2019).

717 41. Olsen, K., Reynolds, K. T. & Hoffmann, A. A. A field cage test of the effects of the
718 endosymbiont *Wolbachia* on *Drosophila melanogaster*. *Heredity* **86**, 731–737 (2001).

719 42. Hamm, C. A. *et al. Wolbachia* do not live by reproductive manipulation alone: Infection
720 polymorphism in *Drosophila suzukii* and *D. subpulchrella*. *Mol. Ecol.* **23**, 4871–4885
721 (2014).

722 43. Ross, P. A. *et al.* Heatwaves cause fluctuations in *w*Mel *Wolbachia* densities and
723 frequencies in *Aedes aegypti*. *PLoS Negl. Trop. Dis.* **14**, e0007958 (2020).

724 44. Ferri, E. *et al.* New insights into the evolution of *Wolbachia* infections in filarial nematodes
725 inferred from a large range of screened species. *PLoS One* **6**, e20843 (2011).

726 45. Zug, R. & Hammerstein, P. Still a host of hosts for *Wolbachia*: Analysis of recent data
727 suggests that 40% of terrestrial arthropod species are infected. *PLoS One* **7**, e38544 (2012).

728 46. Weinert, L. A., Araujo-Jnr, E. V., Ahmed, M. Z. & Welch, J. J. The incidence of bacterial
729 endosymbionts in terrestrial arthropods. *Proc. R. Soc. B Biol. Sci.* **282**, 20150249 (2015).

730 47. O'Neill, S. L., Giordano, R., Colbert, A. M., Karr, T. L. & Robertson, H. M. 16S rRNA
731 phylogenetic analysis of the bacterial endosymbionts associated with cytoplasmic
732 incompatibility in insects. *Proc. Natl. Acad. Sci.* **89**, 2699–2702 (1992).

733 48. Raychoudhury, R., Baldo, L., Oliveira, D. C. & Werren, J. H. Modes of acquisition of
734 *Wolbachia*: Horizontal transfer, hybrid introgression, and codivergence in the *Nasonia*
735 species complex. *Evolution* **63**, 165–183 (2009).

736 49. Conner, W. R. *et al.* Genome comparisons indicate recent transfer of *w*Ri-like *Wolbachia*
737 between sister species *Drosophila suzukii* and *D. subpulchrella*. *Ecol. Evol.* **7**, 9391–9404
738 (2017).

739 50. Gerth, M. & Bleidorn, C. Comparative genomics provides a timeframe for *Wolbachia*
740 evolution and exposes a recent biotin synthesis operon transfer. *Nat. Microbiol.* **2**, 16241
741 (2017).

742 51. Turelli, M. *et al.* Rapid global spread of *w*Ri-like *Wolbachia* across multiple *Drosophila*.
743 *Curr. Biol.* **28**, 963-971.e8 (2018).

744 52. Cooper, B. S., Vanderpool, D., Conner, W. R., Matute, D. R. & Turelli, M. *Wolbachia*
745 acquisition by *Drosophila yakuba*-clade hosts and transfer of incompatibility loci between
746 distantly related *Wolbachia*. *Genetics* **212**, 1399–1419 (2019).

747 53. Shropshire, D. *et al.* Rapid turnover of pathogen-blocking *Wolbachia* and their
748 incompatibility loci. *bioRxiv* 2023–12 (2023).

749 54. Vancaester, E. & Blaxter, M. Phylogenomic analysis of *Wolbachia* genomes from the
750 Darwin Tree of Life biodiversity genomics project. *PLoS Biol.* **21**, e3001972 (2023).

751 55. Caspari, E. & Watson, G. On the evolutionary importance of cytoplasmic sterility in
752 mosquitoes. *Evolution* **13**, 568–570 (1959).

753 56. Turelli, M., Katznelson, A. & Ginsberg, P. S. Why *Wolbachia*-induced cytoplasmic
754 incompatibility is so common. *Proc. Natl. Acad. Sci.* **119**, e2211637119 (2022).

755 57. Turelli, M. & Hoffmann, A. A. Rapid spread of an inherited incompatibility factor in
756 California *Drosophila*. *Nature* **353**, 440–442 (1991).

757 58. Kriesner, P., Conner, W. R., Weeks, A. R., Turelli, M. & Hoffmann, A. A. Persistence of a
758 *Wolbachia* infection frequency cline in *Drosophila melanogaster* and the possible role of
759 reproductive dormancy. *Evolution* **70**, 979–997 (2016).

760 59. Hadfield, S. J. & Axton, J. M. Germ cells colonized by endosymbiotic bacteria. *Nature* **402**,
761 482 (1999).

762 60. Veneti, Z., Clark, M. E., Karr, T. L., Savakis, C. & Bourtzis, K. Heads or tails: host-parasite
763 interactions in the *Drosophila*-*Wolbachia* system. *Appl. Environ. Microbiol.* **70**, 5366–5372
764 (2004).

765 61. Ferree, P. M. *et al. Wolbachia* utilizes host microtubules and Dynein for anterior
766 localization in the *Drosophila* oocyte. *PLoS Pathog.* **1**, e14 (2005).

767 62. Serbus, L. R. & Sullivan, W. A cellular basis for *Wolbachia* recruitment to the host
768 germline. *PLoS Pathog.* **3**, e190 (2007).

769 63. Russell, S. L., Lemseffer, N. & Sullivan, W. T. *Wolbachia* and host germline components
770 compete for kinesin-mediated transport to the posterior pole of the *Drosophila* oocyte.
771 *PLoS Pathog.* **14**, e1007216 (2018).

772 64. Prout, T. Some evolutionary possibilities for a microbe that causes incompatibility in its
773 host. *Evolution* **48**, 909–911 (1994).

774 65. Turelli, M. Evolution of incompatibility-inducing microbes and their hosts. *Evolution* **48**,
775 1500–1513 (1994).

776 66. Hague, M. T., Caldwell, C. N. & Cooper, B. S. Pervasive effects of *Wolbachia* on host
777 temperature preference. *mBio* **11**, e01768-20 (2020).

778 67. Hague, M. T. J., Woods, H. A. & Cooper, B. S. Pervasive effects of *Wolbachia* on host
779 activity. *Biol. Lett.* **17**, 20210052 (2021).

780 68. Pagel, M. Inferring the historical patterns of biological evolution. *Nature* **401**, 877–884
781 (1999).

782 69. Freckleton, R. P., Harvey, P. H. & Pagel, M. Phylogenetic analysis and comparative data: a
783 test and review of evidence. *Am. Nat.* **160**, 712–726 (2002).

784 70. Rajpurohit, S. & Schmidt, P. S. Measuring thermal behavior in smaller insects: A case
785 study in *Drosophila melanogaster* demonstrates effects of sex, geographic origin, and
786 rearing temperature on adult behavior. *Fly (Austin)* **10**, 149–161 (2016).

787 71. Funkhouser-Jones, L. J., van Opstal, E. J., Sharma, A. & Bordenstein, S. R. The maternal
788 effect gene Wds controls *Wolbachia* titer in *Nasonia*. *Curr. Biol.* **28**, 1692–1702 (2018).

789 72. Frydman, H. M., Li, J. M., Robson, D. N. & Wieschaus, E. Somatic stem cell niche tropism
790 in *Wolbachia*. *Nature* **441**, 509 (2006).

791 73. White, P. M. *et al.* Mechanisms of horizontal cell-to-cell transfer of *Wolbachia* spp. in
792 *Drosophila melanogaster*. *Appl Env. Microbiol* **83**, e03425-16 (2017).

793 74. Richardson, M. F. *et al.* Population genomics of the *Wolbachia* endosymbiont in
794 *Drosophila melanogaster*. *PLoS Genet.* **8**, e1003129 (2012).

795 75. Chrostek, E. *et al. Wolbachia* variants induce differential protection to viruses in
796 *Drosophila melanogaster*: a phenotypic and phylogenomic analysis. *PLoS Genet.* **9**,
797 e1003896 (2013).

798 76. Riegler, M., Sidhu, M., Miller, W. J. & O'Neill, S. L. Evidence for a global *Wolbachia*
799 replacement in *Drosophila melanogaster*. *Curr. Biol.* **15**, 1428–1433 (2005).

800 77. Ilinsky, Y. Coevolution of *Drosophila melanogaster* mtDNA and *Wolbachia* genotypes.
801 *PLoS One* **8**, e54373 (2013).

802 78. Early, A. M. & Clark, A. G. Monophyly of *Wolbachia pipientis* genomes within *Drosophila*
803 *melanogaster*: Geographic structuring, titre variation and host effects across five
804 populations. *Mol. Ecol.* **22**, 5765–5778 (2013).

805 79. Strunov, A. *et al.* Historic museum samples provide evidence for a recent replacement of
806 *Wolbachia* types in European *Drosophila melanogaster*. *Mol. Biol. Evol.* **40**, msad258
807 (2023).

808 80. Serbus, L. R. *et al.* A feedback loop between *Wolbachia* and the *Drosophila* gurken mRNP
809 complex influences *Wolbachia* titer. *J. Cell Sci.* **124**, 4299–4308 (2011).

810 81. Poinsot, D., Bourtzis, K., Markakis, G., Savakis, C. & Merçot, H. Wolbachia transfer from
811 *Drosophila melanogaster* into *D. simulans*: Host effect and cytoplasmic incompatibility
812 relationships. *Genetics* **150**, 227–237 (1998).

813 82. Shropshire, J. D., Hamant, E. & Cooper, B. S. Male age and *Wolbachia* dynamics:
814 investigating how fast and why bacterial densities and cytoplasmic incompatibility
815 strengths vary. *mBio* **12**, e02998-21 (2021).

816 83. Hart, B. L. Biological basis of the behavior of sick animals. *Neurosci. Biobehav. Rev.* **12**,
817 123–137 (1988).

818 84. De Roode, J. C. & Lefèvre, T. Behavioral immunity in insects. *Insects* **3**, 789–820 (2012).

819 85. Curtis, V. A. Infection-avoidance behaviour in humans and other animals. *Trends Immunol.*
820 **35**, 457–464 (2014).

821 86. Fedorka, K. M., Kutch, I. C., Collins, L. & Musto, E. Cold temperature preference in
822 bacterially infected *Drosophila melanogaster* improves survival but is remarkably
823 suboptimal. *J. Insect Physiol.* **93**, 36–41 (2016).

824 87. White, P. M. *et al.* Reliance of *Wolbachia* on high rates of host proteolysis revealed by a
825 genome-wide RNAi screen of *Drosophila* cells. *Genetics* **205**, 1473–1488 (2017).

826 88. Grobler, Y. *et al.* Whole genome screen reveals a novel relationship between *Wolbachia*
827 levels and *Drosophila* host translation. *PLoS Pathog.* **14**, e1007445 (2018).

828 89. Chrostek, E. & Teixeira, L. Mutualism breakdown by amplification of *Wolbachia* genes.
829 *PLoS Biol.* **13**, e1002065 (2015).

830 90. Chrostek, E. & Teixeira, L. Within host selection for faster replicating bacterial symbionts.
831 *PLoS One* **13**, e0191530 (2018).

832 91. Duarte, E. H., Carvalho, A., López-Madrigal, S., Costa, J. & Teixeira, L. Forward genetics
833 in *Wolbachia*: Regulation of *Wolbachia* proliferation by the amplification and deletion of
834 an addictive genomic island. *PLOS Genet.* **17**, e1009612 (2021).

835 92. Woolfit, M. *et al.* Genomic evolution of the pathogenic *Wolbachia* strain, <i>w<i/>MelPop.
836 *Genome Biol. Evol.* **5**, 2189–2204 (2013).

837 93. Hoffmann, A. A., Hercus, M. & Dagher, H. Population dynamics of the *Wolbachia*
838 infection causing cytoplasmic incompatibility in *Drosophila melanogaster*. *Genetics* **148**,
839 221–231 (1998).

840 94. Reynolds, K. T. & Hoffmann, A. A. Male age, host effects and the weak expression or non-
841 expression of cytoplasmic incompatibility in *Drosophila* strains infected by maternally
842 transmitted *Wolbachia*. *Genet. Res.* **80**, 79–87 (2002).

843 95. Giordano, R., O'Neill, S. L. & Robertson, H. M. *Wolbachia* infections and the expression
844 of cytoplasmic incompatibility in *Drosophila sechellia* and *D. mauritiana*. *Genetics* **140**,
845 1307–1317 (1995).

846 96. Hoffmann, A. & Turelli, M. Unidirectional incompatibility in *Drosophila simulans*:
847 inheritance, geographic variation and fitness effects. *Genetics* **119**, 435–444 (1988).

848 97. Rousset, F. & Solignac, M. Evolution of single and double *Wolbachia* symbioses during
849 speciation in the *Drosophila simulans* complex. *Proc. Natl. Acad. Sci.* **92**, 6389–6393
850 (1995).

851 98. James, A. C. & Ballard, J. W. O. Expression of cytoplasmic incompatibility in *Drosophila*
852 *simulans* and its impact on infection frequencies and distribution of *Wolbachia pipientis*.
853 *Evolution* **54**, 1661–1672 (2000).

854 99. Ballard, J. W. O. Sequential evolution of a symbiont inferred from the host: *Wolbachia* and
855 *Drosophila simulans*. *Mol. Biol. Evol.* **21**, 428–442 (2004).

856 100. Bourtzis, K., Nirgianaki, A., Markakis, G. & Savakis, C. *Wolbachia* infection and
857 cytoplasmic incompatibility in *Drosophila* species. *Genetics* **144**, 1063–1073 (1996).

858 101. Choi, J. Y., Bubnell, J. E. & Aquadro, C. F. Population genomics of infectious and
859 integrated *Wolbachia pipientis* genomes in *Drosophila ananassae*. *Genome Biol. Evol.* **7**,
860 2362–2382 (2015).

861 102. Osborne, S. E., Leong, Y. S., O'Neill, S. L. & Johnson, K. N. Variation in antiviral
862 protection mediated by different *Wolbachia* strains in *Drosophila simulans*. *PLOS Pathog.*
863 **5**, e1000656 (2009).

864 103. Martinez, J. *et al.* Symbionts commonly provide broad spectrum resistance to viruses in
865 insects: A comparative analysis of *Wolbachia* strains. *PLOS Pathog.* **10**, e1004369 (2014).

866 104. Gu, X. *et al.* A *w*Mel *Wolbachia* variant in *Aedes aegypti* from field-collected *Drosophila*
867 *melanogaster* with increased phenotypic stability under heat stress. *Environ. Microbiol.* **24**,
868 2119–2135 (2022).

869 105. Ballard, J. & Melvin, R. Tetracycline treatment influences mitochondrial metabolism and
870 mtDNA density two generations after treatment in *Drosophila*. *Insect Mol. Biol.* **16**, 799–
871 802 (2007).

872 106. Cooper, B. S., Ginsberg, P. S., Turelli, M. & Matute, D. R. *Wolbachia* in the *Drosophila*
873 *yakuba* complex: Pervasive frequency variation and weak cytoplasmic incompatibility, but
874 no apparent effect on reproductive isolation. *Genetics* **205**, 333–351 (2017).

875 107. R Core Team. *R: A Language and Environment for Statistical Computing*. (R Foundation
876 for Statistical Computing, Vienna, Austria, 2023).

877 108. Canty, C. & Ripley, B. boot: Bootstrap R (S-Plus) functions. (2017).

878 109. Bates, D., Mächler, M., Bolker, B. & Walker, S. Fitting linear mixed-effects models using
879 lme4. *J. Stat. Softw.* **67**, 1–48 (2015).

880 110. Singmann, H., Bolker, B., Westfall, J., Aust, F. & Ben-Shachar, M. S. *Afex: Analysis of*
881 *Factorial Experiments*. (2020).

882 111. Pfaffl, M. W. A new mathematical model for relative quantification in real-time RT–PCR.
883 *Nucleic Acids Res.* **29**, e45–e45 (2001).

884 112. Schneider, C. A., Rasband, W. S. & Eliceiri, K. W. NIH Image to ImageJ: 25 years of
885 image analysis. *Nat. Methods* **9**, 671–675 (2012).

886 113. Klasson, L. *et al.* The mosaic genome structure of the *Wolbachia w*Ri strain infecting
887 *Drosophila simulans*. *Proc. Natl. Acad. Sci.* **106**, 5725–5730 (2009).

888 114. Salzberg, S. L. *et al.* Serendipitous discovery of *Wolbachia* genomes in multiple
889 *Drosophila* species. *Genome Biol.* **6**, R23 (2005).

890 115. Ellegaard, K. M., Klasson, L., Näslund, K., Bourtzis, K. & Andersson, S. G. Comparative
891 genomics of *Wolbachia* and the bacterial species concept. *PLoS Genet.* **9**, e1003381 (2013).

892 116. Seemann, T. Prokka: rapid prokaryotic genome annotation. *Bioinformatics* **30**, 2068–2069
893 (2014).

894 117. Höhna, S. *et al.* RevBayes: Bayesian phylogenetic inference using graphical models and an
895 interactive model-specification language. *Syst. Biol.* **65**, 726–736 (2016).

896 118. Hoskins, R. A. *et al.* The Release 6 reference sequence of the Drosophila melanogaster
897 genome. *Genome Res.* **25**, 445–458 (2015).

898 119. Hu, T. T., Eisen, M. B., Thornton, K. R. & Andolfatto, P. A second-generation assembly of
899 the Drosophila simulans genome provides new insights into patterns of lineage-specific
900 divergence. *Genome Res.* **23**, 89–98 (2013).

901 120. Conner, W. R. *et al.* A phylogeny for the *Drosophila montium* species group: A model
902 clade for comparative analyses. *Mol. Phylogenet. Evol.* **158**, 107061 (2021).

903 121. Clark, A. G. *et al.* Evolution of genes and genomes on the *Drosophila* phylogeny. *Nature*
904 **450**, 203–218 (2007).

905 122. Katoh, K. & Standley, D. M. MAFFT multiple sequence alignment software version 7:
906 improvements in performance and usability. *Mol. Biol. Evol.* **30**, 772–780 (2013).

907 123. Revell, L. J. phytools: an R package for phylogenetic comparative biology (and other
908 things). *Methods Ecol. Evol.* **3**, 217–223 (2012).

909 124. Boettiger, C., Coop, G. & Ralph, P. Is your phylogeny informative? Measuring the power
910 of comparative methods. *Evolution* **66**, 2240–2251 (2012).

911 125. Suvorov, A. *et al.* Widespread introgression across a phylogeny of 155 *Drosophila*
912 genomes. *Curr. Biol.* **32**, 111–123 (2022).

913